

# Novel wholly aromatic polyamide-hydrazide: 3. Preparation and characterization of semiconductors from poly[4-(terephthaloylamino) salicylic acid hydrazide]–metal chelates

Nadia A. Mohamed

Department of Chemistry, Faculty of Science, Cairo University, Giza, Egypt

and Katsuhiko Nakamae\*

Department of Industrial Chemistry, Faculty of Engineering, Kobe University, Rokko, Nada, Kobe 657, Japan

(Received 28 August 1992; revised 21 December 1992)

The effect of the introduction of metal on the physical and electronic properties of a functional polymer, poly[4-(terephthaloylamino)salicylic acid hydrazide], PTASH, has been investigated. Cu(II), Ag(I), Ni(II) and Co(II) chelates of the polymer were prepared. The results revealed that metal ions were chelated with the PTASH repeating unit in a ratio of 1:1. The structure of the resulting chelates was determined by elemental analysis and i.r. spectroscopy. The chelates showed good solubility in several common organic solvents. Thermal gravimetric analysis showed that the chelates are characterized by high thermal and thermo-oxidative stabilities and the degradation temperatures ranged from 510 to 585°C in air and from 555 to 610°C in a nitrogen atmosphere. The chelates were found to become electronic conductors upon treatment with various reducing agents. Their electrical surface resistivities ranged from  $5.3 \times 10^5$  to  $0.5 \times 10^{-2} \Omega \text{ mm}^{-2}$  and were affected by the amount of metal incorporated onto the polymer chains. The electrical conductivities of the reduced chelate films are attributed to the formation of a metallic surface layer by the action of reducing agents. This layer is illustrated not only by the lustrous metallic appearance of the chelate film surfaces but is also confirmed by X-ray diffraction and SEM. Further, all the metal chelates studied here are flexible and possess higher tensile strength than the non-chelated PTASH.

(Keywords: electronic conductors; chelates; preparation)

## INTRODUCTION

In recent years, semiconducting organic polymers have attracted considerable attention for their numerous applications in electronic devices. These polymers can be classified into charge transfer complexes<sup>1,2</sup>,  $\pi$ -electron systems<sup>3,4</sup> and metal chelates<sup>5-14</sup>.

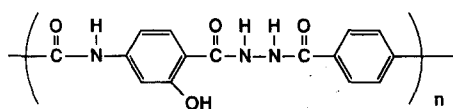
The first successful preparation of polymer–metal chelates was reported in 1964 by Frazer and Wallenberger<sup>15</sup>. They prepared a series of bulk, films and fibres of polyhydrazide–metal chelates but they did not examine their electrical conductivities. Following this work, Hojo *et al.*<sup>5</sup> and Sumita *et al.*<sup>6,7</sup> have studied complex formation of poly(vinyl alcohol) (PVA) with Cu(II) ions in aqueous solution. The former group<sup>5</sup> determined the stability constants of PVA–bivalent metal ion complexes by means of potentiometric titration and investigated the changes in viscosity, solubility, tacticity and other properties of these complexes. Easily processed organic semiconducting polymers were prepared by the modification of Cu(II) chelates of polyacrylamide (PAAm)

and PVA with an acetone solution of iodine<sup>8,9</sup>. Surface resistivities of these chelates were affected by the amount of cupric salt, iodine and the degree of neutralization of the chelate solutions. Further, a method was proposed to prepare a Ag–Hg thin alloy on a PAAm film surface by holding PAAm–AgNO<sub>3</sub> casting solution in a Hg saturated atmosphere. The film conductivity was controlled by the pH of the PAAm solution<sup>10,11</sup>. Recently, a novel method to prepare metallized plastics from metal chelates of PVA, polyamide and copolyamide-imide<sup>12-14</sup> has been reported. These metal chelate films exhibited poor electrical resistivities after their treatment with reducing agents.

Based on the above, it is obvious that both wholly aromatic polyhydrazides and polyamides are able to form metal chelates. Accordingly, this led to the idea that polyamide–hydrazide should be an extremely effective chelating agent. Thus, the present paper discusses the preparation and properties of a series of semiconductors based on poly[4-(terephthaloylamino)salicylic acid hydrazide], PTASH, via its chelation with several transition metal salts.

The preparation and investigation of PTASH have been studied extensively in our laboratory<sup>16,17</sup>. It

\* To whom correspondence should be addressed



Poly[4-(terephthaloylamino)salicylic acid hydrazide]  
PTASH

possesses remarkable thermal and thermo-oxidative stabilities together with chemical resistance and good mechanical properties.

## EXPERIMENTAL

### Materials

PTASH was prepared by a low temperature ( $-5$  to  $-10^{\circ}\text{C}$ ) solution polycondensation reaction of *p*-aminosalicylic acid hydrazide and terephthaloyl chloride in *N,N*-dimethylacetamide (DMAc). A full description of this polymerization procedure has been given previously<sup>16</sup>. The intrinsic viscosity of the prepared polymer is  $4.7 \text{ dl g}^{-1}$ . Silver nitrate ( $\text{AgNO}_3$ ), cupric chloride ( $\text{CuCl}_2$ ), cobalt chloride ( $\text{CoCl}_2$ ) and nickel chloride ( $\text{NiCl}_2$ ) were extra pure anhydrous salts obtained from Nacalai Tesque Inc., Japan. Sodium borohydride ( $\text{NaBH}_4$ ), magnesium (Mg) powder and iron (Fe) powder were used as received from Wako Pure Chemical Industries, Japan.

### PTASH–metal chelate preparation

PTASH–metal chelate was prepared by dissolving a predetermined amount of PTASH (to form 7 wt% solution) and metal salt separately in DMAc. After complete dissolution, the metal salt solution was mixed with the polymer solution and stirred at room temperature overnight. The resulting highly viscous chelate solution was then cast on a dry, clean Pyrex glass plate to a uniform thickness. The plate was placed in an air-circulating electrically heated oven at  $100^{\circ}\text{C}$  for 2 h. Then the plate was immersed in deionized water for 24 h to remove the residual solvent and any unchelated metal salt from the resulting film. Finally, the film was dried at  $100^{\circ}\text{C}$  to constant weight. The metal salts used were  $\text{AgNO}_3$ ,  $\text{CoCl}_2$ ,  $\text{NiCl}_2$  and  $\text{CuCl}_2$ . Their mole fractions were selected between 0.2 and 0.8. All films prepared in this way were 40–45  $\mu\text{m}$  thick, appeared highly coloured and exhibited good mechanical properties. They were kept prior to use in a desiccator over silica gel.

Another method was carried out which involved soaking PTASH film (which was cast from 7 wt% solution in DMAc, thermally treated at  $100^{\circ}\text{C}$  for 2 h, immersed in deionized water overnight and finally dried) in aqueous metal salt solution at  $50^{\circ}\text{C}$  for 2 weeks. The concentrations of metal salts were controlled between 5 wt% and 30 wt%.

PTASH–metal chelate films were reduced according to the method described by Yen *et al.*<sup>12</sup>. The films were treated with various reducing agents for desired periods of time at preselected temperatures. The reducing agents included aqueous  $\text{NaBH}_4$ , Mg powder in dilute hydrochloric acid (HCl) and Fe powder in dilute acetic acid ( $\text{CH}_3\text{COOH}$ ). All the reduced films were washed repeatedly with water and dried in a vacuum oven at  $80^{\circ}\text{C}$  for 48 h to constant weight in order to avoid the contribution of water to the electrical conductivity of the chelate films.

### PTASH–metal chelate identification

I.r. spectra of PTASH–metal chelate films were recorded on a Shimadzu Fourier transform infra-red spectrophotometer (FTIR 4200) in the wavenumber range from 4000 to  $600 \text{ cm}^{-1}$  at  $25^{\circ}\text{C}$ . The investigated chelates were also characterized by elemental analysis. U.v. and visible spectra of the chelates were performed using a Hitachi U-2000 spectrophotometer in the range from 200 to 1000 nm. All the chelates used were unreduced thin films with the same thickness (3  $\mu\text{m}$ ).

### PTASH–metal chelate properties

Electrical resistivity of the reduced chelate films was measured according to the four-probe method using a Takeda Riken electrometer (TR 8651). The surface resistivities were determined and expressed in  $\Omega \text{ mm}^{-2}$ .

The surfaces of PTASH–metal chelate films were observed with a Hitachi scanning electron microscope (model S 2500). The reduced films were examined directly, while the unreduced films were coated with a thin layer of gold prior to being studied.

X-ray diffractograms of the reduced chelates were carried out on a Rigaku RAD-B system with a Ni monochromator. The power level was 40 kV/15 mA with  $\text{CuK}\alpha$  radiation.

Thermal gravimetric analysis (t.g.a.) of PTASH–metal chelates was carried out in air and nitrogen atmospheres. A Daini Seikosha thermal analyser (SSC-560) was used. The sample weights ranged from 10 to 15 mg and the samples were heated from 25 to  $750^{\circ}\text{C}$  at a heating rate of  $10^{\circ}\text{C min}^{-1}$  and under a gas flow stream of  $30 \text{ ml min}^{-1}$ .

Tensile strength, elongation-to-break and elastic modulus of the investigated chelate films were measured on a Shimadzu Autograph in air at room temperature.

Preliminary investigations of the electrical conductivity of PTASH–metal chelates have shown the greater conducting efficiency of the chelates prepared by the mixed method relative to that of those prepared by the soaking method. This may be attributed to the lower ability of metal salt to penetrate into the polymer chains during soaking. For this reason, the present study has been confined to the investigation, elucidation of structure and evaluation of various properties including electrical resistivity of PTASH–metal chelates prepared by the mixed method.

## RESULTS AND DISCUSSION

### Chelate preparation

PTASH–metal chelates were prepared by stirring the mixed DMAc solutions of PTASH and metal salts at room temperature overnight. Mole fractions of the metal salts in both feed solutions and the resulting chelates as well as the percentage of metal in the chelates are presented in Table 1. It can be seen that the obtained chelates have almost the same proportions of metal salt as in the corresponding feed solutions when the mole fractions of metal salts ranged from 0.2 to 0.5. However, from 0.5 to 0.8, an insignificant increase in the mole fractions of metal salts in the resulting chelates was obtained. This indicates that the metal salt is chelated with the PTASH repeating unit in a ratio of 1:1.

**Table 1** Chelation of PTASH with various transition metal salts

Chelate code	Metal salt	Mole fraction of metal salt in feed	Metal in chelate (%)	Mole fraction of metal salt in chelate	Film colour
PTASH-Cu(II)	CuCl <sub>2</sub>	0.3	7.60	0.297	Slight green
		0.5	14.52	0.495	Green
		0.7	17.70	0.569	Green
		0.8	18.30	0.582	Green
PTASH-Ag(I)	AgNO <sub>3</sub>	0.2	7.91	0.199	Slight brown
		0.5	22.89	0.496	Brown
		0.7	25.30	0.536	Dark brown
		0.8	26.84	0.561	Dark brown
PTASH-Co(II)	CoCl <sub>2</sub>	0.2	4.51	0.200	Pale blue
		0.5	13.10	0.481	Blue
		0.7	14.83	0.526	Blue
		0.8	16.48	0.566	Blue
PTASH-Ni(II)	NiCl <sub>2</sub>	0.2	3.98	0.181	Light green
		0.5	13.42	0.491	Green
		0.7	15.09	0.533	Green
		0.8	16.43	0.566	Green

**Table 2** Elemental analysis data of various PTASH–metal chelates and some changes of their i.r. spectra

Chelate code <sup>a</sup>	Elemental analysis (%) <sup>b</sup>				Metal	Main i.r. peaks (cm <sup>-1</sup> )	
	C	H	N	O <sup>c</sup>		C=O	NH, –OH
PTASH	60.53	3.71	14.11	21.65	–	1670–1650	3400–3100
PTASH-Cu(II)	50.15	2.49	11.69	17.97	17.70 (17.72) <sup>d</sup>	1640–1625	3650–3450
PTASH-Ag(I)	44.61	2.46	10.39	15.70	26.84 (26.71)	1635–1630	3620–3500
PTASH-Co(II)	51.03	2.51	11.91	18.07	16.48 (16.65)	1635–1625	3600–3450
PTASH-Ni(II)	51.01	2.52	11.93	18.11	16.43 (16.60)	1655–1640	3590–3360

<sup>a</sup> Only selected data are listed

<sup>b</sup> This showed the absence of chlorine in the prepared Cu(II), Co(II) and Ni(II) chelates

<sup>c</sup> Calculated by difference

<sup>d</sup> Calculated values in parentheses

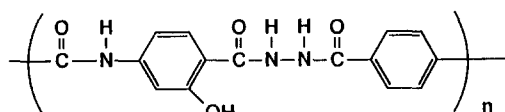
### Chelate structure

The structure of PTASH–metal chelates is proposed on the basis of their elemental analysis and i.r. spectra.

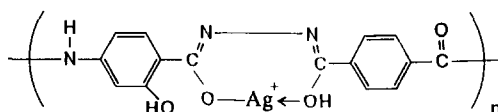
Elemental analysis data of various PTASH–metal chelates together with some changes in i.r. spectra of these chelates are shown in *Table 2*. The i.r. spectrum of non-chelated PTASH showed the presence of three characteristic absorption bands at 3400–3100 cm<sup>-1</sup>, which corresponds to stretching vibrations of >NH combined with phenolic –OH as well as possible interchain hydrogen bonding, at 2200–2100 cm<sup>-1</sup> assigned to enole configurations of hydrazide and amide groups, and at 1670–1650 cm<sup>-1</sup> indicating amide >C=O stretching<sup>16</sup>. All i.r. spectra of various PTASH–metal chelates showed a common shift in the carbonyl absorption band to shorter frequency associated with a reduction in its intensity (*Table 2*). This indicated that a chemical bond between metal ions and carbonyl oxygen may be formed resulting in partial loss of carbonyl double bond character. Further, it could be noted that the intensity of the band due to enole configurations of

hydrazide and amide linkages is increased indicating participation of the enole form of the polymer in coordination. The upward shift of the stretching vibration of the combined >NH, –OH and hydrogen bonding in chelates (*Table 2*) together with a decrease in its intensity confirm almost complete cleavage of the hydrogen bonds and deprotonation of the >NH group. Finally, i.r. spectra showed the appearance of new bands at 1620 cm<sup>-1</sup> (weak) corresponding to the >C=N– stretching vibration<sup>18,19</sup> and at 1020 cm<sup>-1</sup> (–O–C= stretching<sup>20</sup>) as well as at 450 and 570 cm<sup>-1</sup> assigned to the stretching vibrations of M–O and M–N, respectively<sup>21</sup>. The latter bands confirm coordination through the carbonyl oxygen and amide nitrogen.

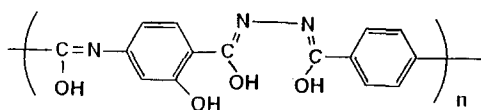
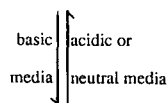
Based on the above results, it thus seems that in basic medium (DMAc) the hydrazide (–CONHNHCO–) and amide (–CONH–) groups, which link the aromatic rings, as shown in **A** (*Scheme 1*), are capable of participating in extended conjugation with the aromatic nuclei through their enole forms, as seen in **B** (*Scheme 1*)<sup>8,15,22–24</sup>. Such conjugation stabilizes the system.



PTASH (Keto form, A)



Structure 4

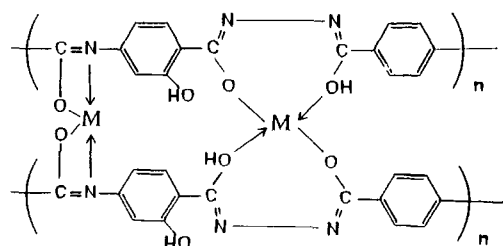


PTASH (enole form, B)

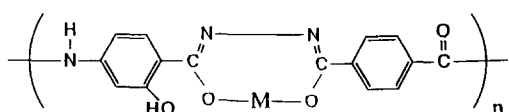
Scheme 1

Thus, the chelation reaction may be proceeded by the chemical interaction between the metal ions and PTASH enole form.

On the basis of the elemental analysis for various bivalent metal chelates, structures 1 and 2 can be deduced.



Structure 1

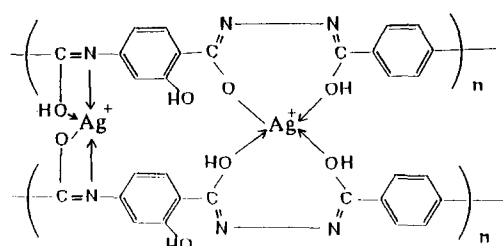


Structure 2

where  $M = \text{Cu(II)}$ ,  $\text{Co(II)}$  or  $\text{Ni(II)}$  ions.

According to i.r. spectral data, the appearance of the metal-nitrogen ( $M-N$ ) band seems to support structure 1.

Similarly, for monovalent metal chelate, two different structures (3 and 4) can be proposed. Structure 3 is the most likely to occur.



Structure 3

Additional experimental proof for the chelation reaction was performed by using u.v.-vis. analysis. It is interesting to note that all PTASH-metal chelates are highly coloured with the colour characterizing the metal ion used as described in Table 1. Visible absorption spectra of various PTASH-metal chelate films are presented in Figure 1. The non-chelated PTASH exhibited an absorption peak at 365 nm (u.v. range) and did not show any absorption in the visible range. However, it showed another absorption peak at 512 nm after chelation with  $\text{Ag(I)}$  ions. The PTASH- $\text{Cu(II)}$  chelate exhibited two absorption peaks at 617 and 463 nm, while the absorption spectral peaks of PTASH- $\text{Co(II)}$  and PTASH- $\text{Ni(II)}$  chelates appear at 689 and 626 nm, respectively. These results indicate that PTASH is able to form chelates with several transition metal salts. This was illustrated not only by producing highly coloured compounds but also by imparting several interesting properties and surface features to the metallized films obtained. This will be discussed later.

#### Chelate properties

All the chelates studied here exhibit good solubility in the same solvents as non-chelated PTASH such as DMAc, dimethyl sulfoxide, *N*-methyl-2-pyrrolidone and dimethyl formamide and can be cast into films. The reduced chelates did not dissolve in the above solvents but were found to dissolve in concentrated mineral acids with degradation. This may be attributed to the transformation of metal ions to the metal upon reduction ( $M^{n+} \rightarrow M^0$ ).

All of the chelates exhibited electrical resistivities of  $\geq 10^{10} \Omega \text{ mm}^{-2}$ . Upon treatment with various reducing

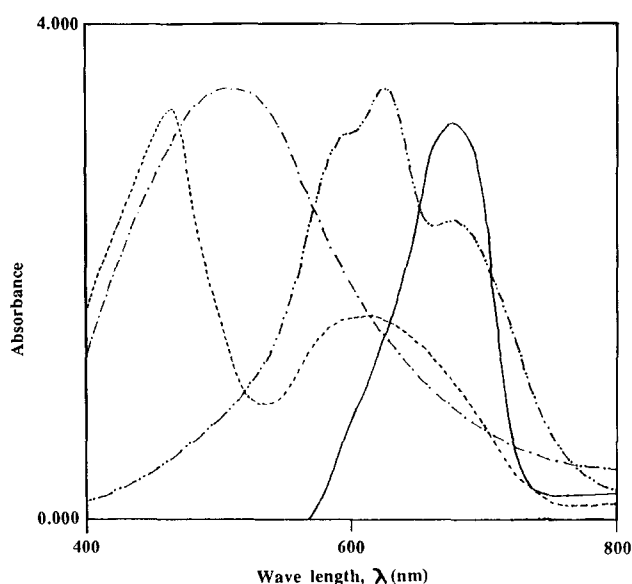


Figure 1 Visible absorption spectra of various PTASH-metal chelate films: (—) PTASH- $\text{Co(II)}$  [13.10% Co]; (---) PTASH- $\text{Cu(II)}$  [14.52% Cu]; (- · -) PTASH- $\text{Ag(I)}$  [22.89% Ag]; (· · ·) PTASH- $\text{Ni(II)}$  [13.42% Ni]

agents, the electrical resistivities significantly fell. The electrical resistivities of PTASH-Cu(II), PTASH-Ag(I), PTASH-Co(II) and PTASH-Ni(II) chelates treated with aqueous NaBH<sub>4</sub>, Mg/HCl and Fe/CH<sub>3</sub>COOH are shown in Tables 3–5, respectively. These tables also illustrate the effect of the metal content of the chelates on their resistivities. It should be noted that all chelates showed a considerable change in colour to a shiny metallic appearance upon treatment with the reducing agents (Table 3). Reduction times were extended from 1 s to 10 min and it was found that after exposure for 2 min to aqueous NaBH<sub>4</sub> solution, saturation reduction had occurred and the minimum electrical resistivity was observed. However, for Mg/HCl and Fe/CH<sub>3</sub>COOH exposure for 30 s was required. The results also demonstrate how the electrical resistivity decreases with increasing metal content of the chelates. For example, in PTASH-Cu chelates, an increase in Cu content from 7.6 to 18.3% resulted in a decrease in the electrical resistivity from  $9.1 \times 10^2$  to  $5.4 \times 10^{-2}$ ,  $5.3 \times 10^3$  to  $2.4 \times 10^{-2}$

**Table 3** Effect of the metal content of various PTASH-metal chelates on their electrical resistivities<sup>a</sup>

Chelate code	Metal <sup>b</sup> (%)	Surface resistivity ( $\Omega \text{ mm}^{-2}$ )	Colour of reduced chelate film
PTASH-Cu	7.60	$9.1 \times 10^2$	Reddish, lustrous
	14.52	$2.5 \times 10^{-1}$	
	17.70	$8.3 \times 10^{-2}$	
	18.30	$5.4 \times 10^{-2}$	
PTASH-Ag	7.91	$4.1 \times 10$	Silvery, lustrous
	22.89	$1.1 \times 10^{-2}$	
	25.30	$0.9 \times 10^{-2}$	
	26.84	$0.8 \times 10^{-2}$	
PTASH-Co	4.51	$7.2 \times 10^4$	Dark grey, lustrous
	13.10	$2.3 \times 10^{-1}$	
	14.83	$3.6 \times 10^{-2}$	
	16.48	$3.9 \times 10^{-2}$	
PTASH-Ni	3.98	$5.3 \times 10^5$	White, lustrous
	13.42	$1.9 \times 10^{-1}$	
	15.09	$8.3 \times 10^{-2}$	
	16.43	$6.4 \times 10^{-2}$	

<sup>a</sup> All chelates were reduced by 3 wt% aqueous NaBH<sub>4</sub> solution at 65°C for 2 min

<sup>b</sup> As determined in elemental analysis

**Table 4** Effect of the metal content of PTASH-metal chelates on their electrical resistivities<sup>a</sup>

Chelate code	Metal (%)	Surface resistivity ( $\Omega \text{ mm}^{-2}$ )
PTASH-Cu	7.60	$5.3 \times 10^3$
	14.52	3.3
	17.70	$3.9 \times 10^{-2}$
	18.30	$2.4 \times 10^{-2}$
PTASH-Ag	7.91	1.1
	22.89	$0.9 \times 10^{-2}$
	25.30	$1.3 \times 10^{-2}$
	26.84	$0.5 \times 10^{-2}$
PTASH-Co	4.51	$5.7 \times 10^2$
	13.10	$2.3 \times 10^{-1}$
	14.83	$1.9 \times 10^{-2}$
	16.48	$0.7 \times 10^{-2}$
PTASH-Ni	3.98	$3.6 \times 10^3$
	13.42	$2.4 \times 10^{-2}$
	15.09	$1.3 \times 10^{-2}$
	16.43	$1.1 \times 10^{-2}$

<sup>a</sup> All chelates were treated with Mg/HCl (1 g Mg in 10 ml of 1% aqueous HCl) at room temperature for 30 s

**Table 5** Effect of the metal content of various PTASH-metal chelates on their electrical resistivities<sup>a</sup>

Chelate code	Metal (%)	Surface resistivity ( $\Omega \text{ mm}^{-2}$ )
PTASH-Cu	7.60	$3.9 \times 10^2$
	14.52	$2.1 \times 10^{-1}$
	17.70	$1.9 \times 10^{-2}$
	18.30	$1.2 \times 10^{-2}$
PTASH-Ag	7.91	2.3
	22.84	$1.3 \times 10^{-2}$
	25.30	$1.1 \times 10^{-2}$
	26.84	$1.5 \times 10^{-2}$
PTASH-Co	4.51	$5.3 \times 10^3$
	13.10	$3.1 \times 10^{-2}$
	14.83	$2.9 \times 10^{-2}$
	16.48	$1.9 \times 10^{-2}$
PTASH-Ni	3.98	$2.7 \times 10^3$
	13.42	$2.8 \times 10^{-2}$
	15.09	$2.8 \times 10^{-2}$
	16.43	$0.9 \times 10^{-2}$

<sup>a</sup> All chelates reduced by Fe/CH<sub>3</sub>COOH (1 g Fe in 10 ml of 2% aqueous CH<sub>3</sub>COOH) at room temperature for 30 s

and  $3.9 \times 10^2$  to  $1.2 \times 10^{-2} \Omega \text{ mm}^{-2}$  after treatment with NaBH<sub>4</sub>, Mg/HCl and Fe/CH<sub>3</sub>COOH, respectively (Tables 3–5).

To understand the action of the reducing agents on the chelate films, the surfaces of various chelate films were observed by SEM before and after their reduction as shown in Figure 2. It can be noted that the non-reduced surfaces are smooth and free of any particles as presented in Figure 2a. Interestingly, the reduced surfaces of the same films appeared rough as a result of a homogeneous aggregation of metal particles covering the whole surface as seen in Figures 2b–e. This reflected the fact that metal ions are distributed uniformly along the polymer chains during the chelation step. Consequently, the reducing agent attacks the parts which are rich in metal chelates resulting in continuous development of metal on the film surface and finally a metallic surface layer will be formed. This layer is most likely responsible for the electrical conductivity of the chelates. When the metal content incorporated into PTASH was small (e.g. 3.98% Ni), the reduced film has poor conductivity due to a discontinuous dispersion of Ni on the film surface as shown in Figure 2f.

In order to obtain more evidence for the metallic surface layer two experiments were carried out using X-ray diffraction. Figure 3 illustrates the diffractograms of PTASH-Cu and PTASH-Ag chelates that had been treated with NaBH<sub>4</sub> and Mg/HCl, respectively. As might be expected, the chelates yielded distinct diffraction peaks (see Table 6). Diffraction peaks of pure Ag and Cu metal are also given in Table 6 for comparison. It can be seen that all the peaks of PTASH-Cu and PTASH-Ag are in excellent agreement with those of pure Cu and Ag metal, respectively. This result, coupled with the SEM observations and the electrical resistivity results, leads us to believe that a metallic surface layer is formed by the action of the reducing agents. This layer is responsible for imparting the electrical conductivity to these chelates.

The thermal stabilities of the chelates were determined using t.g.a. under nitrogen and air atmospheres. Figure 4 shows the thermograms of various chelates. The result for non-chelated PTASH is also shown. The results clearly show the high thermal stabilities of these chelates. Their degradation temperatures were found to vary

between 555°C and 610°C under nitrogen with no weight loss at lower temperatures. When air was used as a t.g.a. atmosphere, stability to 585°C was observed with residues varying between 20 wt% and 56 wt% at 750°C indicative of the different metal oxides formed. Moreover, the results

showed a common behaviour in the decomposition of these chelates.

In addition, the weight loss (6%) which occurred between 300°C and 450°C, due to the cyclodehydration reaction of the non-chelated PTASH hydrazide group into 1,3,4-oxadiazole by losing water (Scheme 2), did not occur for the PTASH-metal chelates. This result would seem to support the proposed chelate structure.

The effect of the introduction of metal onto the polymer chains on its mechanical properties was also examined. Both the tensile strength and the elastic modulus of PTASH were improved after chelation with Cu(II), Ag(I), Co(II) and Ni(II) ions as seen in Table 7. However, the

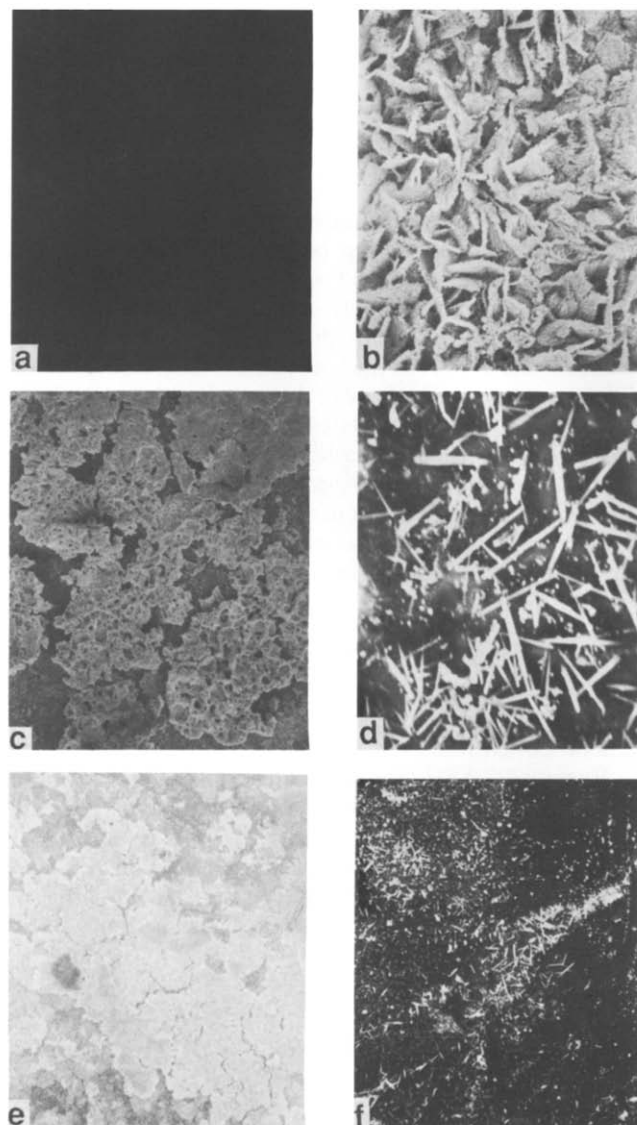


**Figure 2** Scanning electron micrographs of various PTASH-metal chelates: (a) PTASH-Ag(I) [26.84% Ag] unreduced; (b) PTASH-Ag [26.84% Ag] reduced by Mg/HCl; (c) PTASH-Cu [18.30% Cu] reduced by aqueous NaBH<sub>4</sub>; (d) PTASH-Ni [15.09% Ni] reduced by Fe/CH<sub>3</sub>COOH; (e) PTASH-Co [16.48% Co] reduced by Mg/HCl; (f) PTASH-Ni [3.98% Ni] reduced by Fe/CH<sub>3</sub>COOH

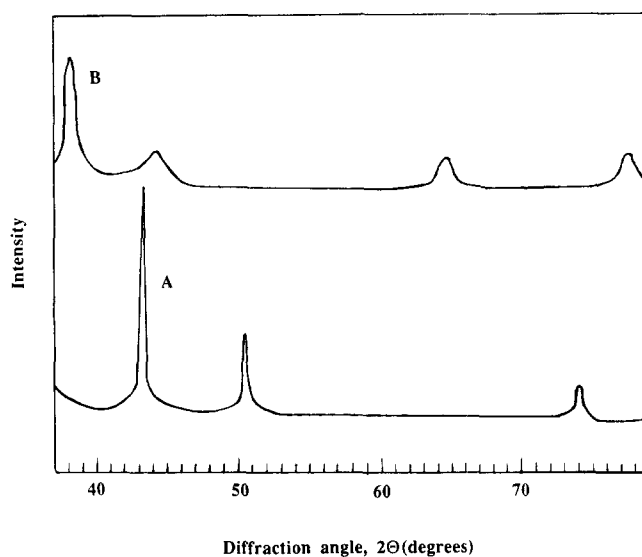
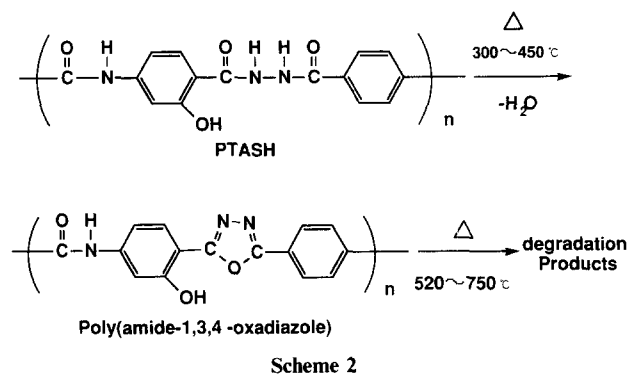


**Figure 3** X-ray diffraction patterns for PTASH-metal chelates: (A) PTASH-Cu [17.70% Cu] reduced by NaBH<sub>4</sub>; (B) PTASH-Ag [25.30% Ag] reduced by Mg/HCl

**Table 6** Summary of X-ray diffraction results for various PTASH-metal chelates<sup>a</sup>

PTASH-Cu (17.70% Cu)		Pure Cu metal <sup>b</sup>		PTASH-Ag (25.30% Ag)		Pure Ag metal <sup>b</sup>	
2θ (deg)	d (Å)	2θ (deg)	d (Å)	2θ (deg)	d (Å)	2θ (deg)	d (Å)
43.4	2.084	43.30	2.088	38.14	2.359	38.14	2.359
50.5	1.807	50.43	1.808	44.20	2.049	44.33	2.043
74.2	1.278	74.13	1.278	64.62	1.442	64.50	1.445
				77.55	1.231	77.61	1.230

<sup>a</sup> 2θ, diffraction angles; d, plane distance of the peaks observed in X-ray analysis

<sup>b</sup> These data were taken from reference 12

**Table 7** Mechanical properties of various PTASH-metal chelate films before and after treatment with aqueous NaBH<sub>4</sub> solution<sup>a</sup>

Chelate code	Unreduced			Reduced		
	<i>T</i> (MPa)	<i>E</i> (%)	<i>M</i> (GPa)	<i>T</i> (MPa)	<i>E</i> (%)	<i>M</i> (GPa)
PTASH	205.80	44.00	4.21	—	—	—
PTASH-Ag (26.84% Ag)	311.32	29.23	4.90	333.62	28.67	4.75
PTASH-Cu (18.30% Cu)	298.51	28.60	4.61	299.12	29.41	4.72
PTASH-Ni (15.09% Ni)	301.19	28.70	4.12	305.81	27.90	4.06
PTASH-Co (16.48% Co)	263.93	39.40	4.15	259.43	32.90	3.78

<sup>a</sup> *T*, tensile strength; *E*, elongation-to-break; *M*, elastic modulus. The reduction conditions are as described in Table 3

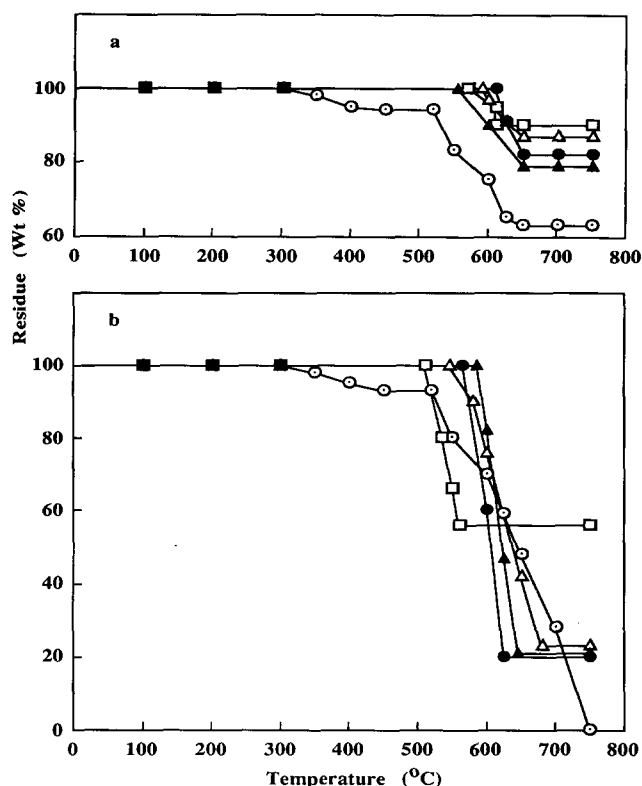


**Figure 4** Thermal gravimetric analysis of various PTASH-metal chelates in (a) nitrogen and (b) air: (○) non-chelated PTASH; (□) PTASH-Ag(I) [25.30% Ag]; (△) PTASH-Cu(II) [17.70% Cu]; (●) PTASH-Ni(II) [15.09% Ni]; (▲) PTASH-Co(II) [14.83% Co]

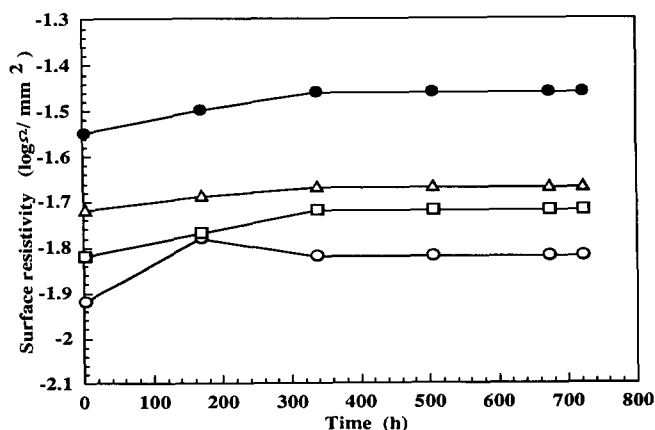


**Figure 5** Effect of ambient environment on the surface resistivity of various PTASH-metal chelates. All chelates films were reduced by Fe/CH<sub>3</sub>COOH: (○) PTASH-Cu [18.30% Cu]; (□) PTASH-Ag [26.84% Ag]; (△) PTASH-Co [16.48% Co]; (●) PTASH-Ni [15.09% Ni]

elongation-to-break decreased. This may be attributed to the partial crosslinking between the polymer chains upon chelation (proposed structures 1 and 3). From Table 7, it can be seen that the tensile strength, elongation-to-break and the elastic modulus of the reduced chelate films did not show any considerable differences relative to those of the unreduced chelate films.

Finally, the reduced chelates exhibit good environmental stability. The effect of ambient environment on the electrical resistivity of various PTASH-metal chelates is shown in Figure 5. The results revealed that no significant change in the electrical resistivity of these chelates was observed during storage in an ambient environment for 720 h.

## CONCLUSIONS

Based on the above results one may arrive at the following general conclusions.

1. Various PTASH-metal chelates having different metal contents were successfully prepared as film-forming solutions.
2. The introduction of various transition metals onto PTASH has been utilized to improve its physical properties and to impart electrical conductivity to the resulting chelates.
3. PTASH-metal chelates were found to become conductors upon treatment with reducing agents.
4. The prepared chelates possess two attractive features: first, their ready processability due to their high ability to dissolve in several amide solvents; and second, the stability of the reduced chelate films towards air and moisture.
5. Another advantage of the chelation of PTASH is that its mechanical and thermal properties could be improved markedly.

## REFERENCES

1. Jiang, Z. and Sen, A. *Macromolecules* 1992, **25**, 880
2. Ruiz, J. P., Dharia, J. R., Reynolds, J. R. and Buckley, L. J. *Macromolecules* 1992, **25**, 849
3. Walton, T. R. and Gratz, R. F. *J. Appl. Polym. Sci.* 1992, **44**, 387
4. Shirakawa, H., Louis, E. T., MacDermid, A. G., Chiang, C. K. and Heeger, A. J. *J. Chem. Soc. Chem. Commun.* 1977, 578
5. Hojo, N., Shirai, H. and Hayashi, S. *J. Polym. Sci. Symp.* 1974, **47**, 299
6. Sumita, O., Fukuda, A. and Kuze, E. *J. Polym. Sci., Polym. Phys. Edn* 1978, **16**, 1801
7. Sumita, O., Fukuda, A. and Kuze, E. *J. Appl. Polym. Sci.* 1979, **23**, 2279
8. Higashi, F., Cho, C. S., Kakinoki, H. and Sumita, O. *J. Polym. Sci., Polym. Chem. Edn* 1977, **15**, 2303
9. Higashi, F., Cho, C. S., Kakinoki, H. and Sumita, O. *J. Polym. Sci., Polym. Chem. Edn* 1979, **17**, 313

- 10 Lee, J. Y., Tanaka, H., Takezoe, H., Fukuda, A., Kuze, K. and Iwanaga, H. *J. Appl. Polym. Sci.* 1984, **29**, 795
- 11 Lee, Y. J., Ohtsuka, K., Takezoe, H., Fukuda, A., Kuze, E. and Iwanaga, H. *J. Appl. Polym. Sci.* 1984, **29**, 3813
- 12 Yen, C. C., Chang, T. C. and Kakinoki, H. *J. Appl. Polym. Sci.* 1990, **40**, 5
- 13 Yen, C. C., Huang, C. J. and Chang, T. C. *J. Appl. Polym. Sci.* 1991, **42**, 439
- 14 Huang, C. J., Yen, C. C. and Chang, T. C. *J. Appl. Polym. Sci.* 1991, **42**, 2267
- 15 Frazer, A. H. and Wallenberger, F. T. *J. Polym. Sci.* 1964, **A2**, 1825
- 16 Nadia, A. M. and Nakamae, K. *J. Appl. Polym. Sci., Appl. Polym. Symp. ISPAC-5 Symp. Vol.* in press
- 17 Nakamae, K. and Nadia, A. M. *J. Appl. Polym. Sci., Appl. Polym. Symp. ISPAC-5 Symp. Vol.* in press
- 18 Culbertson, B. M. and Murphy, R. *J. Polym. Sci., Polym. Lett. Edn* 1967, **5**, 807
- 19 Culbertson, B. M. and Murphy, R. *J. Polym. Sci., Polym. Lett. Edn* 1966, **4**, 249
- 20 Frazer, A. H., Sweeny, W. and Wallenberger, F. T. *J. Polym. Sci.* 1964, **A2**, 1157
- 21 Thamizharasi, S. and Reddy, A. V. R. *Eur. Polym. J.* 1992, **28**, 119
- 22 Stolle, R. and Benrath, A. *J. Prakt. Chem.* 1904, **70**, 263
- 23 Benrath, A., Giesler, P. and Gartner, O. *J. Prakt. Chem.* 1924, **107**, 211
- 24 Frazer, A. H. and Wallenberger, F. T. *J. Polym. Sci.* 1964, **A2**, 1147